

# Comparison of magnetic properties of austenitic stainless steel after ion irradiation

Chaoliang Xu\*, Xiangbing Liu, Fei Xue, Yuanfei Li, Wangjie Qian

Suzhou Nuclear Power Research Institute, Suzhou, Jiangsu Province 215004, China

## ARTICLE INFO

### Keywords:

Austenitic stainless steel  
Irradiation  
Magnetization  
Martensite  
Coercivity

## ABSTRACT

Specimens of austenitic stainless steel (ASS) were irradiated with H, Fe and Xe ions at room temperature. The vibrating sample magnetometer (VSM) and grazing incidence X-ray diffraction (GIXRD) were used to analyze the magnetic properties and martensite formation. The magnetic hysteresis loops indicated that higher irradiation damage causes more significant magnetization phenomenon. Under the same damage level, Xe irradiation causes the most significant magnetization, Fe irradiation is the second, and H irradiation is the least. A similar martensite amount variation with irradiation can be obtained. The coercivity  $H_c$  increases first to 2 dpa and then decreases continuously with irradiation damage for Xe irradiation. At the same damage level, H irradiation causes a largest  $H_c$  and Xe irradiation causes a minimal one.

## 1. Introduction

Austenitic stainless steels (ASS) are generally used as incore structural components in light water reactors as internals, neutron flux thimble tube and so on due to its excellent corrosion resistance in combination with high ductility and toughness at elevated temperature. The reliability and integrity of such ASS components are of particular importance for reactors safe operation. However, in-service inspection of the core internals has revealed a susceptibility of baffle to former bolts known as Irradiation Assisted Stress Corrosion Cracking (IASCC). IASCC corresponds to irradiation induced or enhanced intergranular stress corrosion cracking of the material. It is known that corrosion resistance along grain boundaries can be degraded with Cr depletion caused by radiation induced segregation (RIS), and this is considered one of the principle mechanisms of IASCC on stainless steels [1]. Previously Kodama et al. [2] suggested that the IASCC susceptibility was related to the austenite stability in ASS. Simultaneously many studies [3] have indicated that RIS will result in the formation of magnetic phase in austenitic steels. So the investigation of the magnetic phase in ASS can provide information for understanding of IASCC mechanism.

Due to the difficulty on neutron irradiation studies, charged particles (protons and heavy ions) were chosen to simulate the irradiation behaviors of neutron irradiation. So it is critical to understand the difference of magnetic properties and austenitic phase stability in ASS under different ions irradiation. But so far few studies have been carried out due to the limitation of shallow penetration depth of ions irradiation which leads to a difficulty to obtain the magnetic properties from a

thicker unirradiated layer.

In the present studies, the vibrating sample magnetometer (VSM) was conducted with a TEM specimen to investigate the magnetic properties under H, Fe and Xe. The saturated magnetization and coercivity obtained from hysteresis loops were give a detailed analysis and comparison subsequently with the irradiation damage and damage rate. Moreover, in order to give more auxiliary information of martensite formation in austenite, the grazing incidence X-ray diffraction (GIXRD) was also used.

## 2. Experiments

The materials used in this study are a Z6CND17.12 ASS. The specimens used in experiments were cut from a bar with solution treatment at  $1060 \pm 10$  °C for 90 min. The chemical composition is Cr (17.28%), Ni (11.65%), Mo (2.49%), Mn (1.24%), Cu (0.46%), Si (0.340%), C (0.038%), Co (0.010%), P (0.008%), S (0.003%) and Fe (the balance).

The specimens before irradiation were polished to mirror-like with mechanical method. Then they were irradiated with proton, Fe and Xe ions separately at room temperature to different fluences (as shown in Table 1) at the ECR-320 kV High-voltage Platform in the Institute of Modern Physics. The theoretical results of the displacement damage are calculated by the Monte-Carlo code SRIM 2012 [4] as shown in Table 1, taking the density of  $7.8 \text{ g/cm}^3$  and threshold displacement energies of 40 eV for Fe, Cr and Ni sub-lattices [5]. In the SRIM calculation process, the vacancy file obtained by the Kinchin-Pease quick calculation model was used to calculate the displacement damage values.

\* Corresponding author.

E-mail address: [xuchaoliang@cgnpc.com.cn](mailto:xuchaoliang@cgnpc.com.cn) (C. Xu).

**Table 1**  
The irradiation parameters of ASS specimens.

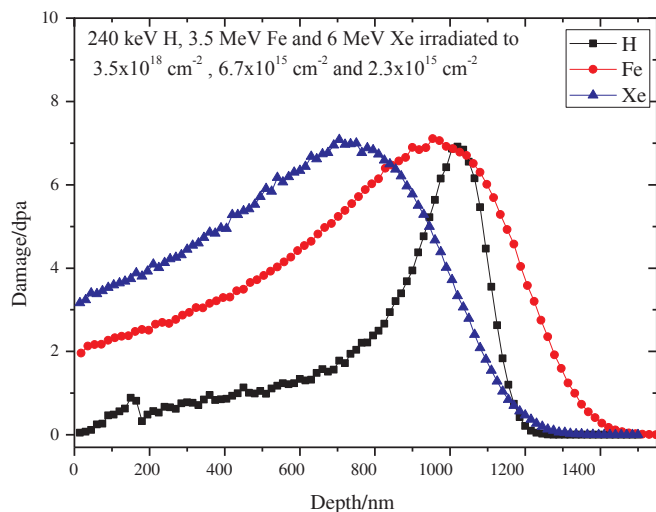
Ions species	Ions energy	Fluence (ions/cm <sup>2</sup> )	Peak displacement damage (dpa)
proton	240 keV	$3.5 \times 10^{18}$	7
Fe	3.5 MeV	$6.7 \times 10^{15}$	7
Xe	6 MeV	$6.6 \times 10^{14}$	2
		$2.3 \times 10^{15}$	7
		$5.0 \times 10^{15}$	15
		$8.3 \times 10^{15}$	25

Magnetic hysteresis loops of ASS were measured with the vibrating sample magnetometer (VSM) 7407 produced by Lake Shore. The maximum magnetic field intensity is 3000 Oe in measurement. A 3 mm diameter disk shape specimens with a thickness of about 30  $\mu$ m was used in measurement to deviate the demagnetizing effects due to specimen shape and size and decrease the effect of unirradiated parts. GIXRD was carried out at Beijing Synchrotron Radiation Facility, Institute of High Energy Physics. X-rays was generated by a bending magnet, focused and monochromated to a wavelength of 0.154 nm. The X-ray scanning range was from 35 to 55 degree with a resolution of 0.05 degree.

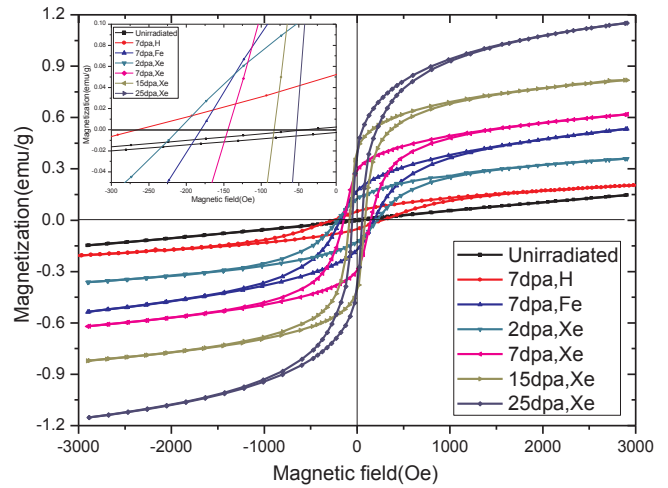
### 3. Results

Fig. 2 shows the variations of magnetization-magnetic field hysteresis loops of initial specimen and specimens irradiated with H, Fe and Xe ions separately to different damage. As shown in Fig. 2, the initial specimen remains a small magnetization in the entire field, showing up no hysteresis dependence typical of ferromagnetic materials. The ASS is paramagnetic due to its perfect austenitic microstructure. The dependence of the specific magnetization  $M$  on the external magnetic field  $H$  for the unirradiated specimen is a straight line described by the dependence of  $M(H) = \chi_p H$ , where  $\chi_p$  is the paramagnetic susceptibility. So there is no hysteresis dependence of unirradiated specimen.

Nevertheless, after irradiation with H, Fe or Xe, the specimens show the hysteresis dependence typical of a ferromagnetic property with a nonlinear variation. For the Xe irradiated specimen, higher irradiation damage causes more significant magnetization. Under the same damage level, Xe irradiation causes the most significant magnetization, Fe irradiation is the second, and H irradiation is the least.



**Fig. 1.** Distribution of displacement damage versus depth in stainless steel irradiated with H, Fe and Xe ions separately to different fluences according to simulation with SRIM.



**Fig. 2.** Variations of hysteresis loops of ASS irradiated with H, Fe and Xe to different damage.

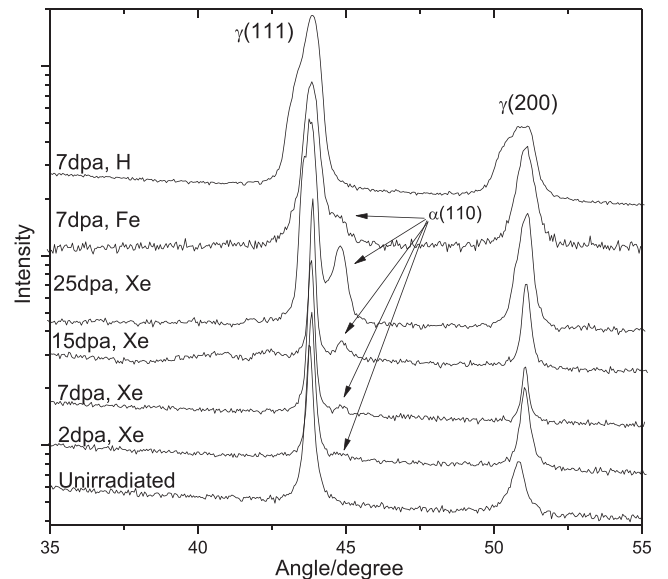


**Fig. 3.** GIXRD patterns of the ASS irradiated with H, Fe and Xe to different damage.

In order to obtain further information of magnetic phase after irradiation, the GIXRD patterns of unirradiated specimen and specimens irradiated to different damage level with H, Fe and Xe were investigated (as shown in Fig. 3). It is observed that the unirradiated specimen shows two face-centered-cubic austenite diffraction peaks of  $\gamma(111)$  and  $\gamma(200)$ . No other diffraction peaks are observed. With increasing the irradiation fluence by Xe, a new diffraction peak corresponding to the  $\alpha(110)$  appears and then become remarkable gradually with irradiation damage increased to 25 dpa. This indicates the formation of  $\alpha$  martensite phase during Xe ion irradiation and the amount of the martensite shows a continuous increase with irradiation. A similar diffraction peak of  $\alpha(110)$  can also be observed after irradiated to 7 dpa by Fe, which also indicate the formation of the martensite. This  $\alpha$  martensite phase has been proved in ASS after ions irradiation by GIXRD [6,7], TEM [8,9] and Mössbauer [10]. Whereas, in the case of H irradiation, compared to the Xe and Fe irradiation, no remarkable new diffraction peak was observed. But the initial  $\gamma(111)$  and  $\gamma(200)$  become broadening.

The austenitic phase exhibits paramagnetic properties and magnetic phase is ferromagnetic. The formation of  $\alpha$  magnetic phase in austenitic

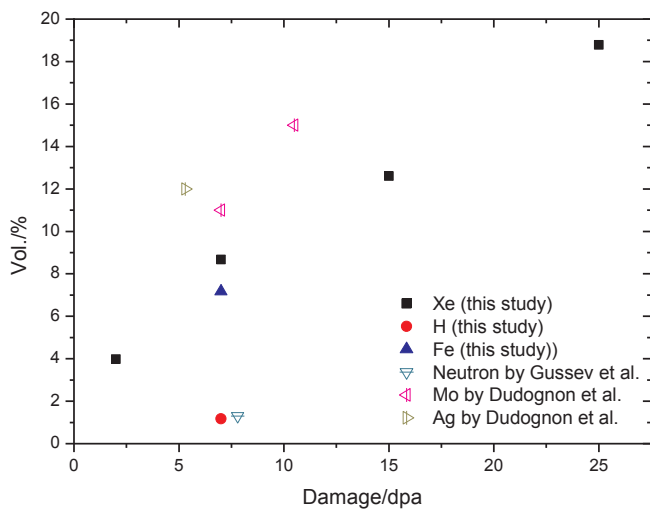


Fig. 4. The variations of ferrite amount for ASS irradiation with H, Fe and Xe to different damage.

has been proved by GIXRD in Fig. 3. Hence, the paramagnetic ASS will become ferromagnetic after irradiation [8]. Previously, Takaya et al. [11] indicated that the saturation magnetization ( $M_s$ ) depends entirely on the amount of the magnetic phase. This suggests that  $M_s$  is a structure-insensitive parameter and the volume amount of martensite phase can be deduced by analysis  $M_s$  [12]. Usually, the more the martensite phase, the higher the  $M_s$ . To evaluate the amount of martensite phase, the  $M_s$  of irradiated specimens can be obtained by subtracting the paramagnetic contribution. We usually take the  $M_s$  of 100 vol% martensite to be about 127 emu/g for 316 stainless steel [13]. Then the calculated martensite amount  $V_M$  can be obtained by  $V_M = (M_{si} - M_{su})/127$ , where the  $M_{si}$  and  $M_{su}$  is the  $M_s$  for irradiated and unirradiated specimens. As shown in Fig. 4, it is indicated that the amount of martensite increases with irradiation damage for Xe irradiated specimens. This proves that the formation of martensite phase is proportional to the irradiation damage. Moreover, under the same damage level, Xe irradiation cause the most martensite, Fe irradiation is the second, and H irradiation is the least. Moreover, previous TEM studies [9] indicated that the volume amount of martensite in ASS after neutron irradiated to 7.8 dpa is about 1.3%, which is closed to volume amount after proton in our study. In addition, XRD analysis indicated that the ASS irradiated with Mo and Ag will result in volume amount of martensite about 11% and 15% (7 and 10.5 dpa with Mo) and 12% (5.3 dpa with Ag) [14], which also approximate our calculated results after Xe irradiation. This proves the correctness of calculation results on martensite above.

Previous studies suggest that there are two different mechanisms for formation of martensite in ASS, namely: martensitic transformation of austenite to martensite of the same composition and nucleation and growth of martensite of different composition than the parent austenite [15].

For the austenitic structure transformation into martensite, it is assumed that irradiation will cause high residual stresses which may be caused by lattice damage [16]. Heavier ions will cause more severe cascade collision comparing to light ions and induce high residual stresses within the lattice, resulting in the more significant structure transformation owing to releasing the high levels of stresses. In fact, considering the differences in damage profile and ion energy, the magnetization actually depends on the energies of PKA (primary knock-on atom). In addition, the structure transformation is also induced by the formation of the highly pressurized Xe bubbles. The pressurized bubbles generate very large shear stresses with a high density in stainless steel, which would tend to assist the phase transformation. So based on the analysis above, more martensite will be formed in ASS by

Xe ions at the same damage level. Together, RIS may cause chemical elements migration and create an environment which is benefit for the formation of martensite [17]. Morisawa et al. [3] further indicated that the mass of the phase transformation by RIS would increase with increasing irradiation damage. So under these two effects, martensite is formed and is proportional to irradiation damage.

On the other hand, Xe irradiation produces a near-uniform distribution of atomic displacement damage (the ratio of minimum and maximum damage is about 50% from the surface to peak damage region), whereas protons produce a remarkable nonuniform distribution of displacement damage with a steep peak at the end of the projective range, as shown in Fig. 1. If the average damage level (over the whole projective ranges of ion-damaged layer) is used instead of the peak damage level, the average damage level of Xe irradiation is largest, Fe irradiation is the second and H irradiation is the least. This behavior is similar to the variation of martensite amount for H, Fe and Xe irradiation. So the irradiation damage distribution is also an important factor affecting the martensite amount analysis.

Coercivity  $H_c$ , the magnetic field where magnetization reaches to zero, can be determined from the hysteresis loops. It is used as a structure-sensitive parameter that is strongly affected by the magnetic phase and dislocation density [18]. Fig. 5 is the variations of  $H_c$  of ASS irradiated with different ions. It is indicated that the  $H_c$  increase first to 2 dpa and then decrease continuously with irradiation damage after Xe irradiation. Under the same damage level, H irradiation causes the largest  $H_c$ , Fe irradiation is the second, and Xe irradiation is the least.

The variation of  $H_c$  under different conditions has been reported in many studies, but the variation trends may increase or decrease after irradiation or deformation [19–22]. Whereas in our study,  $H_c$  increases first and then decreases continuously with irradiation damage. We believe that defects within a domain wall tend to anchor the wall in order to decrease the wall area. Consequently, the domain walls are attracted to the defects which effectively impede wall motion, leading to the increase in the coercivity. Thus, increasing dislocation density will result in an increased coercivity [23]. This conclusion is consistent with the studies of Park et al. [24], O'Sullivan et al. [22] and Hilzinger et al. [25]. Further increase of irradiation damage will cause the growth of magnetic phase size and formation of new magnetic phase. Therefore interaction between the martensite clusters will arise. These interactions will allow the magnetization of one cluster to affect the magnetization of its neighbors, and therefore should change the magnetic properties. Under such situation,  $H_c$  is inversely proportional to the ferrite phase size and cause the decrease of  $H_c$  with irradiation increase due to the domain wall pinning at the grain boundaries when the

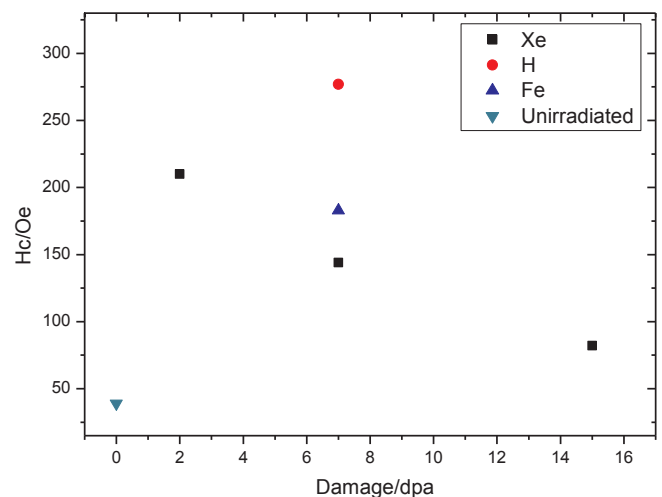


Fig. 5. Variations of  $H_c$  with irradiation damage for unirradiated specimen and specimens irradiated with H, Fe and Xe.

cluster size exceeds the domain wall width [26].

It is indicated that H irradiation causes the largest  $H_c$  and Xe irradiation causes the least one after irradiated to 7 dpa. This phenomenon may be caused by the following reasons. On the one hand, we should pay attention to the different damage rate of H, Fe and Xe, that is a higher damage rate of Xe irradiation ( $8.0 \times 10^{-4}$  dpa/s), a middle damage rate of Fe irradiation ( $4.0 \times 10^{-4}$  dpa/s) and a lower damage rate of proton irradiation ( $1.1 \times 10^{-4}$  dpa/s). In a case of H irradiation, a smaller damage rate results in a lower density of defects per unit time and interaction between radiation induced defects will occur less frequently [27]. Thus the residual surviving simple defects will be higher because the absolute point defect flux to sinks is lower. This can be proved by Fig. 3 where a significantly broadening of  $\gamma(111)$  and  $\gamma(200)$  diffraction peak after H irradiation suggesting a larger defect density [28]. Thus due to a high density of simple defects under low damage rate, a larger  $H_c$  can be obtained. On the other hand, less martensite will be introduced by H irradiation as shown in Fig. 4, so the martensite clusters exceeding the domain wall width will be weak and its effect on decreasing the  $H_c$  will not be significant. Therefore, by synthesizing these two effects, H irradiation causes the largest  $H_c$ , Fe irradiation is the second, and Xe irradiation is the least under the same damage level.

#### 4. Conclusion

ASS specimens were irradiated with H, Fe and Xe ions at room temperature and then vibrating sample magnetometer (VSM) and grazing incidence X-ray diffraction (GIXRD) were carried out to analyze the magnetic properties and martensite formation. The magnetic hysteresis loops indicated that higher irradiation damage causes more significant magnetization phenomenon. Under the same damage level, Xe irradiation causes the most significant magnetization, Fe irradiation is the second, and H irradiation is the least. A similar martensite amount variation with irradiation can also be deduced and the amount of martensite is closed related to the irradiation damage level and ions specimens. The coercivity  $H_c$  was obtained from magnetic hysteresis loops. It is indicated that  $H_c$  increase first to 2 dpa and then decrease continuously with irradiation damage for Xe irradiation. At the same damage level, H irradiation causes a largest  $H_c$  and Xe irradiation causes a minimal one. The different contribution of irradiation defects and martensite phase on  $H_c$  can explain this variation.

#### Acknowledgements

This research is supported by the National Key Research and

Development Program of China (grant No. 2016YFB0700401), the National Natural Science Foundation of China (grant Nos. 11675123 and 11775255) and Natural Science Foundation of Jiangsu Province, China (grant BK20171222).

The authors would like to thank the 320 kV High-voltage Platform in Institute of Modern Physics for ion irradiation experiments and Beijing Synchrotron Radiation Facility, Institute of High Energy Physics for the help on GIXRD.

#### References

- [1] Yoshiyuki Nemoto, Satoshi Keyakida, Tetsuya Uchimoto, et al., *Int. J. Appl. Electromagnet. Mech.* 35 (2011) 123–139.
- [2] M. Kodama, K. Fukuya, H. Kayana, *ASTM-STP 1175* (1994) 889–901.
- [3] J. Morisawa, M. Otaka, M. Kodama, et al., *J. Nucl. Mater.* 302 (2002) 66–71.
- [4] J.P. Biersack, L.G. Hagmark, *Nucl. Instrum. Methods* 174 (1980) 257–269.
- [5] ASTM 521-96, *Standard Practice for Neutron Radiation Damage Simulation by Charged Particle Irradiation*, (2003).
- [6] N. Mottu, M. Vayer, R. Erre, *Surf. Coat. Technol.* 183 (2004) 165–173.
- [7] I. Sakamoto, N. Hayashi, H. Tanoue, *Surf. Coat. Technol.* 65 (1994) 133–136.
- [8] Darya Alontseva, Oleg Maksimkin, Alyona Russakova, *Mater. Sci.* 20 (2014) 15–20.
- [9] M.N. Gussev, J.T. Busby, L. Tan, et al., *J. Nucl. Mater.* 448 (2014) 294–300.
- [10] I. Sakamoto, N. Hayashi, T. Toriyama, *Hyperfine Interact.* 80 (1993) 1019–1024.
- [11] Shigeru Takaya, Ichiro Yamagata, Shoichi Ichikawa, et al., *Int. J. Appl. Electromagnet. Mech.* 33 (2010) 1335–1342.
- [12] Lefu Zhang, Seiki Takahashi, Yasuhiro Kamada, *Ser. Mater.* 57 (2007) 711–714.
- [13] E. Menendez, J. Sort, M.O. Liedke, et al., *J. Mater. Res.* 24 (2009) 565–573.
- [14] J. Dudognon, M. Vayer, A. Pineau, R. Erre, *Surf. Coat. Technol.* 203 (2008) 180–185.
- [15] J.T. Stanley, K.R. Garr, *Metall. Trans. A* 6 (1975) 531–535.
- [16] Rongshan Wang, Xu. Chaoliang, Xiangbing Liu, et al., *J. Nucl. Mater.* 457 (2015) 130–134.
- [17] Wen-Jen Liu, Ji-Jung Kai, Chuen-Horng Tsai, et al., *J. Nucl. Mater.* 212–215 (1994) 476–481.
- [18] P.K. Amitava Mitra, P.K. De Srivastava, et al., *Metall. Mater. Trans. A* 35A (2004) 559–605.
- [19] J. Ding, H. Huang, P.G. McCormick, *J. Magn. Magn. Mater.* 139 (1995) 109–114.
- [20] K. Mumtaz, S. Takahashi, J. Echigoya, et al., *J. Mater. Sci.* 39 (2004) 85–97.
- [21] S.S.M. Tavares, M.R. Da Silva, J.M. Neto, et al., *J. Magn. Magn. Mater.* 1391 (2002) 242–245.
- [22] D. O'Sullivan, M. Cotterell, I. Meszaros, *NDT&E Int.* 37 (2004) 265–269.
- [23] R.A. Taylor, J.P. Jakubovics, *J. Magn. Magn. Mater.* 31–34 (1983) 970–972.
- [24] Duck-Gun Park, Jun-Hwa Hong, In-Sup Kim, et al., *J. Mater. Sci.* 32 (1997) 6141–6146.
- [25] H.R. Hilzinger, H. Kronmuller, *J. Magn. Magn. Mater.* 2 (1976) 11–171.
- [26] J. Manjanna, S. Kobayashi, Y. Kamada, et al., *J. Mater. Sci.* 43 (2008) 2659–2665.
- [27] Christopher D. Hardie, Ceri A. Williams, Xu. Shuo, et al., *J. Nucl. Mater.* 439 (2013) 33–40.
- [28] B.A. Kamalapurkar, S.K. Dubey, A.D. Yadav, *Nucl. Instr. Meth. B* 211 (2003) 383–388.